HOW MUCH OF THE MANTLE MELTS IN A GIANT IMPACT? S. T. Stewart[1], S. J. Lock[2], S. Mukhopadhyay[1]. [1]Department of Earth and Planetary Sciences, U. California, Davis, CA (sts@ucdavis.edu). [2]Department of Earth and Planetary Sciences, Harvard University, Cambridge, MA.

Introduction: The giant impact stage of planet formation is characterized by punctuated deposition of mass and energy on a growing planet. The total energy of accretion is sufficient to completely melt a planet; however, the energy is not evenly distributed in the impact process.

Recent geochemical data from the deep mantle are evidence that the Earth was not completely mixed during accretion [1, 2]. In addition, Tucker & Mukhopadhyay [3] argue for multiple partial mantle magma oceans during Earth's accretion based on differences in He/Ne data from ocean island and mid-ocean ridge basalts. These observations therefore require that the Earth was not completely mixed by giant impacts. Given the rapid overturn times of magma oceans, the most straightforward way to avoid mixing is for part of the planet to remain solid through giant impact events.

Because the spatial deposition of impact energy is extremely sensitive to the details of the impact scenario, the magnitude of melting during giant impact events is difficult to predict. Here, we present results on the spatial heterogeneity of the initial shock energy deposition and discuss the challenges in determining the final melt volume.

Initial Shock Melting Calculations: We simulated the propagation of the impact shock through the target and projectile in 3D using the CTH shock physics code [4]. The planets were hydrodynamic and differentiated with 2000 K potential temperature mantle adiabats with a conductive profile to a solid surface. The giant impact parameter space is described in [5]. Using Lagrangian tracer particles, we determined the peak shock pressure distribution through the mantle. For each parcel of mantle, we estimated the shock pressure necessary to reach the solidus upon decompression to the parcel's pre-impact pressure. Thus, this calculation neglects processes that occur at later times: e.g., decompression melting of a portion of the mantle and secondary impacts.

The estimated mantle melt fraction from the passage of the initial shock reflects the spatial heterogeneity of the shock pressure field. As in the analysis for the atmospheric loss [5, 6], the results are presented vs. a modified specific impact energy,

$$Q_S = Q_R \left(1 + M_p / M_t\right)\left(1 - b\right), \qquad (1)$$

where M_t and M_p are the target and projectile masses, respectively, and Q_R is the specific energy defined in [7]. To calculate the specific impact energy for the projectile, the mass ratio is reversed in Eq. 1.

Heterogeneous Shock Energy Deposition: In grazing impact events, the center of the projectile misses the target ($b > R_t/(R_t+R_p)$, where R_t and R_p are the radii of the target and projectile). In this case, only a portion of the kinetic energy of the projectile is deposited in the target via the impact shock. Because the contact volume between the two bodies is small, the volume of target that experiences high shock pressures is small. Thus, grazing impacts (black points in Fig. 1A) melt only a portion of the target by the initial shock wave.

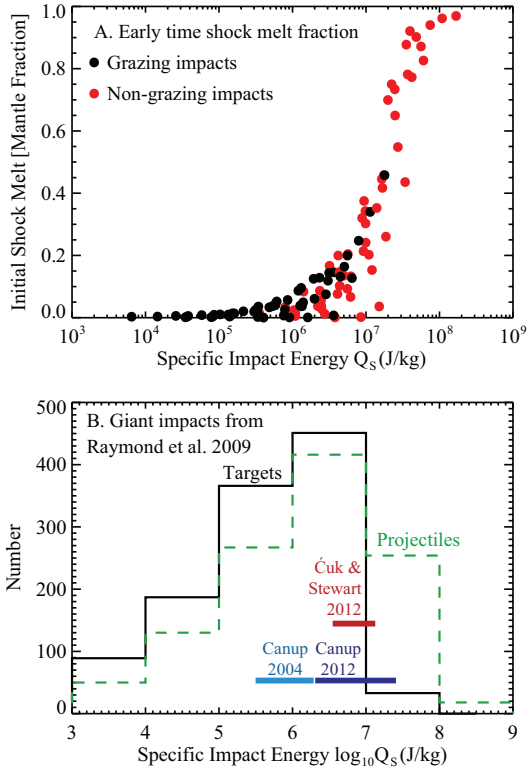

Fig. 1. A. Estimate of the minimum volume of mantle melted by the initial shock wave vs. specific impact energy. The impact energy required for widespread shock melting will be less for targets with higher initial mantle potential temperatures than considered here. Later time processes are neglected to illustrate the limited deposition of shock energy at early times during a giant impact. **B.** Distributions of specific impact energies for all giant impacts from [8]. The impact energy ranges for different Moon-formation scenarios are shown as horizontal bars [9-11].

In contrast, if the impact is non-grazing, most of the projectile's kinetic energy is coupled into the impacted hemisphere of the target. For head-on impacts by small projectiles, most of the kinetic energy is de-

posited as internal energy in the projectile and the impacted hemisphere of the target. In such cases, the projectile and impacted hemisphere may partially vaporize while the antipode hemisphere does not melt from the initial shock.

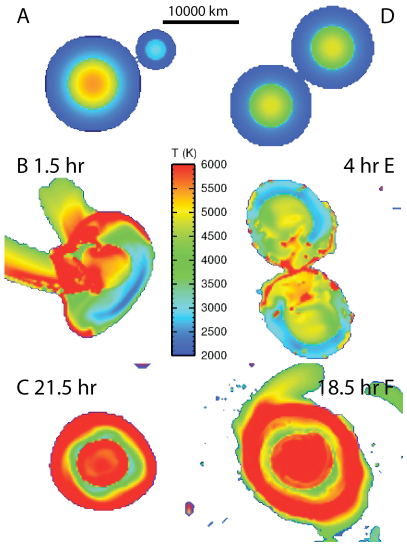

Fig. 2. Equatorial slices of the temperature field during two potential Moon-forming giant impacts of comparable energy but different impact geometries [10, 11]. **A-C.** M_p=0.05M_{Earth}, M_t=0.9M_{Earth}, b=0.5, V_i=2V_{esc}, Q_s=4 × 10^6 J/kg. **D-F.** M_p=0.5M_{Earth}, M_t=0.5M_{Earth}, b=0.7, V_i=1V_{esc}, Q_s=2 × 10^6 J/kg. The absolute temperatures are not robust because of the lack of latent heat of melting in the equations of state, but the calculation illustrates the heterogeneous energy distribution and preservation of a partially solid lower mantle (near the solidus) in both cases (green layers).

The impact heating during two potential Moon-forming impact scenarios are shown in Fig. 2. In Fig. 2A-C, shortly after the initial contact, the contrast between the temperatures in the impacted and antipode hemisphere is dramatic (Fig. 2B). As the planet re-equilibrates, the less buoyant material from the antipode sinks to form the post-impact lower mantle and the post-impact planet is stably stratified (Fig. 2C).

For comparison, consider a graze-and-merge event of similar specific impact energy (Fig. 2D-F). The first grazing contact heats one hemisphere (Fig. 2E). The head-on second impact occurs in the hot hemispheres, preserving the colder mantle material that becomes the post-impact lower mantle. Thus, even high-energy Moon-forming events may not fully melt the Earth.

Late time energy budget and mixing: These calculations do not capture all the details of the energy deposition and mixing at later times during the impact event. Because the antipode hemispheres rarely melt from the initial shock (Fig. 1B), gravitational re-equilibration must include the residual strength of a portion of the mantle. Shear heating during gravitational re-equilibration could raise the temperature of the antipode mantle to the solidus.

Nakajima & Stevenson [12] suggested that the high angular momentum Moon-forming scenarios [10, 11] would lead to complete mantle mixing by Kelvin-Helmholtz instabilities. They state that the Richardson number (*Ri*, half the ratio of potential energy to kinetic energy) is <0.25 for these events. For a shear flow between two invicid stably stratified fluids with *Ri*<0.25, runaway growth of instabilities leads to mixing. However, portions of the mantle are initially solid or partially molten during the shear flows during gravitational re-equilibration and the criteria of *Ri*<0.25 does not apply. In addition, *Ri* varies widely in space and time; thus a single *Ri* value cannot represent an entire impact event. In our calculations, *Ri* is greater than 0.25 in the partially solid lower mantle. The extent of mantle mixing after the impact remains an open question.

The potential energy of core formation may contribute additional energy after an impact event if the projectile's core is deposited within the mantle. However, non-grazing differentiated projectiles penetrate directly to the core of the target in the giant impact regime. In hit-and-run events, the core of the projectile does not accrete. The projectile core is disrupted during a fraction of graze-and-merge type events and the fragments may be small enough to be deposited within the mantle, where potential energy may be released later by segregation to the core. Thus, heating from core formation has a limited effect in the phase space of giant impacts.

Conclusions: Impact energy is deposited heterogeneously. Planetary mantles may have remained partially solid throughout the giant impact stage of planet formation, including the Moon-forming event. Incomplete melting and mixing of mantles during accretion is consistent with recent data showing that the mantle preserves chemical heterogeneities that were generated during Earth's formation.

Acknowledgements: This work was supported by NASA grant #NNX11AK93G (STS), NSF grant #0929193 (SM), NESSF grant #NNX13AO67H (SJL).

References: [1] Mukhopadhyay, S. (2012) *Nature* **486**, 101. [2] Touboul, M., et al. (2012) *Science* **335**, 1065. [3] Tucker, J.M. and S. Mukhopadhyay (2014) *EPSL* **393**, 254. [4] McGlaun, J.M., et al. (1990) *Int. J. Impact Eng.* **10**, 351. [5] Stewart, S.T., et al. (2014) *LPSC* **45**, 2869. [6] Lock, S.J., et al. (in prep.) *EPSL*. [7] Leinhardt, Z.M. and S.T. Stewart (2012) *ApJ* **745**, 79. [8] Raymond, S.N., et al. (2009) *Icarus* **203**, 644. [9] Canup, R.M. (2004) *Icarus* **168**, 433. [10] Canup, R.M. (2012) *Science* **338**, 1052. [11] Ćuk, M. and S.T. Stewart (2012) *Science* **338**, 1047. [12] Nakajima, M. and D.J. Stevenson (2013) *LPSC* **44**, 2680.